LC-PHSM-2001-054

Measurement of the Higgs Boson Mass and Cross Section with a Linear e^+e^- Collider

P. Garcia-Abia*, W. Lohmann† and A. Raspereza†

*CERN [1], EP Division, J21300, CH–1211–Geneva 23, Switzerland
†DESY Zeuthen, Platanenallee 6, D–15738–Zeuthen, Germany

Abstract. The potential of a linear e^+e^- collider operated at a centre-of-mass energy of about 350 GeV is studied for the measurement of the Higgs boson mass and production cross section. An integrated luminosity of 500 fb^{-1} is assumed. For Higgs boson masses of 120, 150 and 180 GeV the uncertainty on the Higgs boson mass measurement is estimated to be 40, 50 and 70 MeV, respectively. The Higgs boson production cross section can be measured in the same mass range with a relative uncertainty between 1% and 3%.

INTRODUCTION

In the Standard Model [1] particles acquire mass due to spontaneous symmetry breaking by introducing one scalar doublet field. The so called Higgs mechanism [2] leads to one remnant scalar particle, the Higgs boson. The mass of the Higgs boson is a free parameter of the Standard Model and of fundamental nature. Once it is determined from experiment the profile of the particle can be predicted. The measurement of the production cross section allows to determine the couplings to gauge bosons. Together with the decay branching fractions the couplings to several fermions or gauge bosons are accessible allowing to prove the structure of the higgs sector.

EXPERIMENTAL CONDITIONS AND DETECTOR SIMULATIONS

The study is performed for a linear collider operated at a center-of-mass energy of 350 GeV and an event sample corresponding to an integrated luminosity of 500 fb^{-1}.

---

1) On leave from the Institut für Physik der Universität Basel, Switzerland.

TABLE 1. The cross section (in fb) times the branching ratio of the signal final states for Higgs boson masses of 120, 150 and 180 GeV as predicted in the Standard Model.

Decay mode	topology	120	150	180
recoil mass	2ℓ + X	10.8	8.3	6.0
$\mathrm{ZH} \to \ell^+\ell^-\mathrm{q\bar{q}}$	2ℓ + 2-jets	8.1	1.7	0.04
$\mathrm{ZH} \to \mathrm{q\bar{q}b\bar{b}}$	4-jets	80.0	16.8	0.4
$\mathrm{ZH} \to \ell^+\ell^-\mathrm{W^+W^-},\ \mathrm{W^\pm} \to \mathrm{q\bar{q}'}$	2ℓ + 4-jets	0.6	2.6	2.6
$\mathrm{ZH} \to \mathrm{q\bar{q}W^+W^-},\ \mathrm{W^\pm} \to \mathrm{q\bar{q}'}$	6-jets	6.0	26.5	26.6
$\mathrm{ZH} \to \mathrm{X}$		160.3	123.7	89.0

The detector used in the simulation follows the proposal for the TESLA collider presented in the Conceptual Design Report [3]. The interaction region is surrounded by a central tracker consisting of a silicon microvertex detector as the innermost part and a time projection chamber. In radial direction follow an electromagnetic calorimeter, a hadron calorimeter, the coils of a superconducting magnet and an instrumented iron flux return yoke. The solenoidal magnetic field is 3T. The central tracker momentum resolution is

$$\frac{\sigma_{p_t}}{p_t} = 7 \cdot 10^{-5} \cdot p_t \text{ [GeV]}, \tag{1}$$

where p_t is the transverse momentum.

The energy resolutions of the electromagnetic and hadronic calorimeters are:

$$\frac{\sigma_{E_{el}}}{E_{el}} = \frac{10\%}{\sqrt{E_{el}}} + 0.6\% \qquad\qquad \frac{\sigma_{E_h}}{E_h} = \frac{50\%}{\sqrt{E_h}} + 4\%, \tag{2}$$

where E_{el} and E_h are the energies measured for electrons and hadrons in the corresponding calorimeters. The polar angular coverage of the central tracker maintaining the resolution is $|\cos\theta| < 0.85$, above this range the tracking resolution detoriates. The electromagnetic and hadron calorimeters cover $|\cos\theta| < 0.996$ maintaining the resolution over the whole angular range. The simulation of the detector is done using SIMDET [4].

PHYSICS PROCESSES

At the centre-of-mass energy considered the dominant process for Higgs boson production in the Standard Model is $\mathrm{e^+e^-} \to \mathrm{Z\,H}$. Events of this process, hereafter refered to as signal, are generated using PYTHIA [5] for Higgs boson masses, m_{H}, of 120, 150 and 180 GeV. The Z decays into electrons, muons and quarks are considered. For the Higgs boson all decay modes are simulated as expected in the Standard Model. The decay modes into $\mathrm{b\bar{b}}$ and $\mathrm{W^+W^-}$ are investigated in detail. The Standard Model cross sections and the expected numbers of events are given in Table 1.

For background estimations events are generated with PYTHIA for the processes $e^+e^- \to (\gamma\gamma) \to e^+e^- f\bar{f}$, $e^+e^- \to f\bar{f}(\gamma)$, $e^+e^- \to W^+W^-$ and $e^+e^- \to ZZ$ and EXCALIBUR [6] for $e^+e^- \to Ze^+e^-$, $e^+e^- \to Z\nu\bar{\nu}$ and $e^+e^- \to W^+e^-\bar{\nu}$.

Initial state Bremsstrahlung is simulated by PYTHIA. Beamstrahlung is taken into account using the CIRCE program [7].

METHODS OF THE MEASUREMENTS AND RESULTS

The least model dependent technique for the measurements of the Higgs boson production cross section, $\sigma(\mathrm{ZH})$, is to use the spectrum of the recoil mass against the Z [8]. The Z decays into electrons and muons are well suited for this purpose, albeit the decay branching fractions are small. Furthermore, the recoil mass spectrum yields also a measurement of m_{H}.

A kinematic fit imposing energy and momentum conservation improves the resolution in $\ell^+\ell^- + 2$-jet and 4-jet final states, hence the accuracy of the mass measurement becomes higher. For 4-jet final states the tagging of b-quarks enlarges substantially the signal to noise ratio.

For Higgs boson masses above 150 GeV, the $\mathrm{H} \to \mathrm{W}^+\mathrm{W}^-$ decay becomes dominant, leading to $\ell^+\ell^- + 4$-jet and 6-jet final states. For their study, jet identification and kinimatic fitting are crucial. In order to construct the covariance matrix used in the kinematic fit, the uncertainties of the lepton and jet energy and angular measurements are needed. For the leptons the tracker resolution from equation (1) is used. The uncertainties of the jet energy and angular measurements are obtained from a Monte Carlo study using the subdetector resolutions from equations (1) and (2). They are parametrised as: $\frac{\sigma_E}{E} = \frac{20\%}{\sqrt{E}}$, $\sigma_\theta = 10$ mrad and $\sigma_\phi = \frac{10 \text{ mrad}}{\sin\theta}$, where E is the energy, θ the polar and ϕ the azimuthal angle of the jet.

The recoil mass

To measure the cross section of $e^+e^- \to \mathrm{Z\,H}$, the decays of the Z into electrons and muons, $\mathrm{Z} \to e^+e^-$ and $\mathrm{Z} \to \mu^+\mu^-$, are exploited. These final states exibit a clean signature in the detector, hence they are easily selected. The selection efficiencies are found to be independent of the decay mode of the Higgs boson. The spectrum of the recoil mass, m_{R}, against the Z,

$$m_{\mathrm{R}}^2 = s - 2 \cdot \sqrt{s} \cdot E_{\mathrm{Z}} + m_{\mathrm{Z}}^2 \tag{3}$$

is used to detect the Higgs boson and to measure its production cross section. Here E_{Z} and m_{Z} are the energy and the mass of the Z.

Electrons are identified as energy deposits in the electromagnetic calorimeter whose shape corresponds to the expectation for an electromagnetic shower and with a matched track in the central tracker. The measured track momentum and

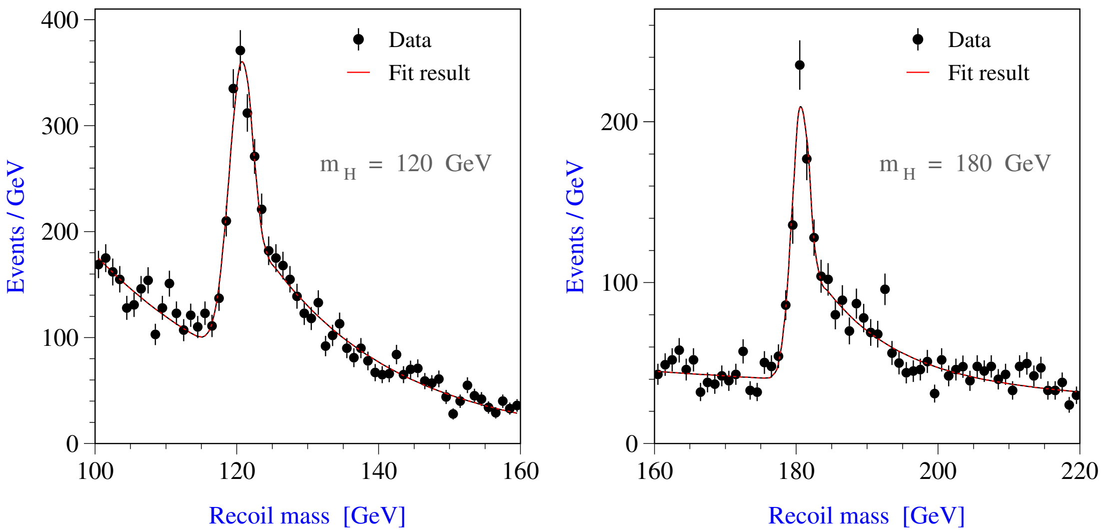

FIGURE 1. The recoil mass spectra off the Z in $e^+e^- \rightarrow$ Z H $\rightarrow \ell^+\ell^-$X for $m_{\rm H}$ =120 GeV (left) and $m_{\rm H}$ =180 GeV (right).

shower energy must be in agreement within 5% and the shower leakage into the hadron calorimeter must be less than 2 GeV. Muons are identified as tracks pointing to energy deposits in the calorimeters which are consistent with the expectation for a minimum ionizing particle. Both electrons and muons must have momenta larger than 10 GeV and fulfil the polar angle cut $|\cos\theta| < 0.9$. The invariant mass of the leptons is required to be within 5 GeV equal to the Z mass. To suppress background from $e^+e^- \rightarrow$ ZZ, the production polar angle of the two-lepton system must be $|cos\theta_{ll}| < 0.6$. The selection efficiencies for the processes $e^+e^- \rightarrow$ Z H $\rightarrow e^+e^-$X and $\mu^+\mu^-X$ are about 50%, nearly independent on $m_{\rm H}$. The recoil mass distributions obtained for the superposition of signal and background are shown in Figure 1 for $m_{\rm H}$ = 120 GeV and 180 GeV combining the final states $e^+e^- \rightarrow$ Z H $\rightarrow e^+e^-$X and $\mu^+\mu^-X$. The Higgs boson appears well on top of a small and smooth background. The latter results mainly from $e^+e^- \rightarrow$ ZZ[2].

The recoil mass spectra are fitted with a superposition of the signal and background distributions. The signal is parametrised with a gaussian. To account for its asymmetric shape the upper side tail is approximated as the sum of a gaussian and an exponential function. The fit of the mass has an error of 110 MeV at $m_{\rm H}$ =120 GeV and 95 MeV at $m_{\rm H}$ = 180 GeV, the accuracy of the cross section measurement results to $\Delta\sigma/\sigma$ = 2.6 % and 3.8 %, respectively.

---

[2] It has been pointed out [9] that the background resulting from Bhabha scattering is underestimated when using PYTHIA as compared to BHWIDE [10]. We have verified that the total background in Figure 1 is about 20% larger using BHWIDE. This amount is significantly reduced after a cut on the energy of a radiative photon in the event, without affecting the signal.

The ZH $\rightarrow \ell^+\ell^-\mathrm{q\bar{q}}$ and ZH $\rightarrow \mathrm{q\bar{q}b\bar{b}}$ final states

These final states are characterised by two isolated leptons and two jets or four jets. Leptons are identified as described in the previous section. Tracks and calorimetric energy deposits not classified as isolated leptons are grouped into jets using the Cambridge [11] and Durham [12] jet clustering algorithms. The events are subject of a kinematic fit [13] imposing energy and momentum conservation. In addition, for 4-jet final states the invariant mass of the two jets assigned to the Z decay is fixed to m_{Z}.

For the ZH $\rightarrow \ell^+\ell^-\mathrm{q\bar{q}}$ final state the dijet invariant mass spectra after the 4C fit are shown in Figure 2 for m_{H} = 120 GeV and 150 GeV, respectively.

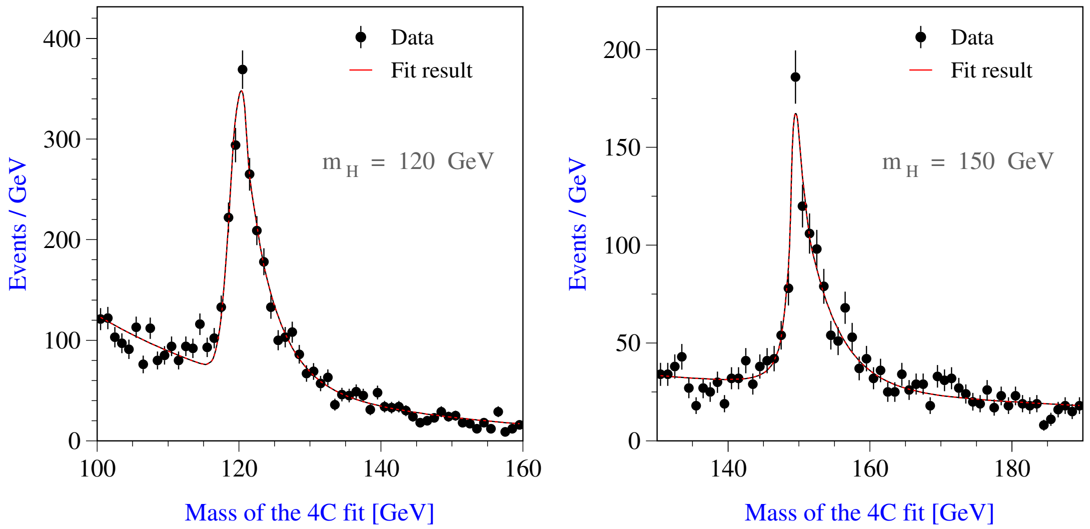

FIGURE 2. The dijet invariant mass from the ZH $\rightarrow \ell^+\ell^-\mathrm{q\bar{q}}$ final state after a 4C kinematic fit for m_{H} = 120 GeV (left) and 150 GeV (right).

The mass obtained from the fit has an error of 70 MeV at m_{H} =120 GeV and 90 MeV at m_{H} = 150 GeV. The accuracy of the cross section measurement results to $\Delta\sigma/\sigma$ = 3.0 % and 4.7 %, respectively.

In the 4-jet sample, the signal is enhanced using the event b-tag [14], which quantifies the number of jets, for which a b-quark decay is detected. The effect of requiring at least one or two jets tagged as a b-quark decay is shown in Figure 3. The distribution of the invariant mass of the jets assigned to the Higgs boson after the 5C kinematic fit is shown in Figure 4 for m_{H} = 120 GeV. accepting only events with at least two jets tagged as b-quark decay.

The fit of the mass has an error of 45 MeV at m_{H} =120 GeV and 170 MeV at m_{H} = 150 GeV. The accuracy of the cross section measurement results to $\Delta\sigma/\sigma$ = 1.1 % and 3.4 %, respectively.

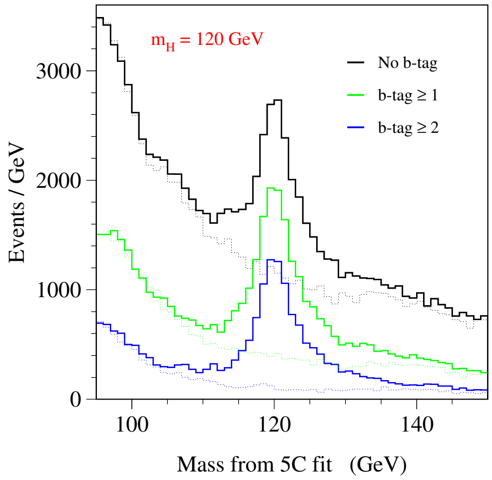

FIGURE 3. The invariant mass of the two jets assigned to the Higgs boson decay in the $\mathrm{ZH} \to \mathrm{q\bar{q}b\bar{b}}$ final state with no requirement on b-tag, at least one jet and at least two jets tagged as b decay.

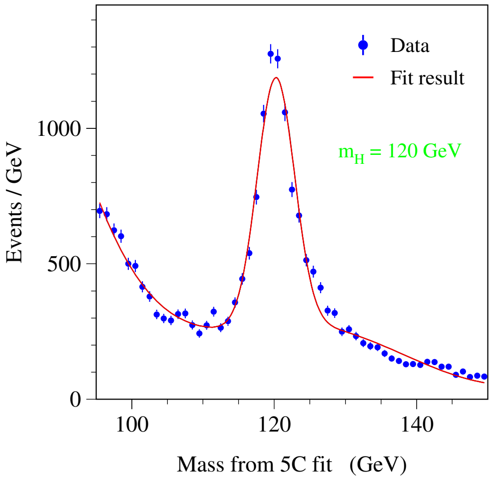

FIGURE 4. The invariant mass of the two jets assigned to the Higgs boson decay in the $\mathrm{ZH} \to \mathrm{q\bar{q}b\bar{b}}$ final state after a 5C kinematic fit for m_H = 120 GeV. At least two jets are required to be tagged as b-quark decay.

The $\mathrm{ZH} \to \ell^+\ell^-\mathrm{W^+W^-}$ and $\mathrm{ZH} \to \mathrm{q\bar{q}W^+W^-}$ final states

We consider W-boson decays into two quarks, hence the topologies of these final states are two isolated leptons and four or six jets. The requirements for electron and muon identification are the same as in the previous section.

Details of the analysis of these final states are given in Reference [15]. Events of the process $\mathrm{ZH} \to \ell^+\ell^-\mathrm{W^+W^-}$ are selected by requiring high multiplicity in the tracking device and the calorimeters, the energy deposited in the detector to be greater than 85% of the centre-of-mass energy and two isolated electrons or muons. Furthermore the global event shape variables thrust and the second Fox-Wolfram moment [5] are used to suppress the dominant background from the WW and ZZ final states. The values of the cuts depend on the Higgs boson mass hypothesis and are more stringent at m_H = 120 GeV than at m_H = 180 GeV. In the same Higgs boson mass range the selection efficiency for signal events varies from 25% to 72%. The two leptons of $\mathrm{ZH} \to \ell^+\ell^-\mathrm{W^+W^-}$ are expected to stem from the Z. Requiring their invariant mass to be within 10 GeV equal to m_Z the background is suppressed considerably. Tracks and calorimetric energy deposits not stemming from the leptons are grouped into four jets using the Durham algorithm. Then a 4C kinematic fit is performed imposing energy and momentum conservation. The 4-jet invariant mass distributions are shown in Figure 5 for m_H = 150 GeV and m_H = 180 GeV, respectively.

The mass distributions are fitted using a modified gaussian as in the previous sections. The uncertainty of the mass amounts to about 100 MeV for both mass values and the uncertainty of the cross section to 5.2% and 4% for m_H = 150 and

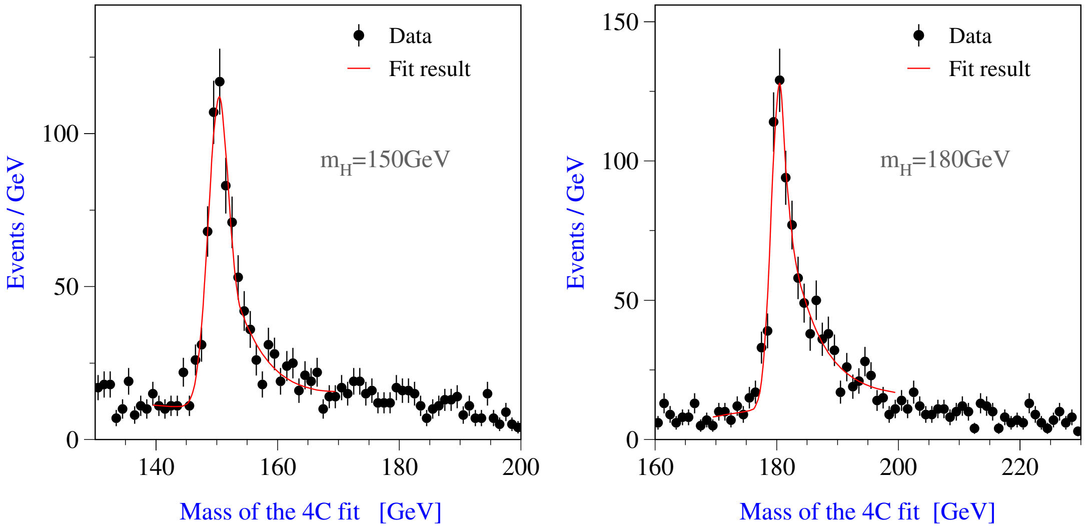

FIGURE 5. The 4-jet invariant mass from the ZH $\rightarrow \ell^+\ell^-\mathrm{W}^+\mathrm{W}^-$ final state after a 4C kinematic fit for m_H = 150 GeV (left) and 180 GeV (right).

180 GeV, respectively.

The ZH $\rightarrow \mathrm{q\bar{q}W^+W^-}$ channel is selected first by requiring high-multiplicity events with a total energy deposits in the detector greater than 80% of the centre-of-mass energy. The event thrust must be less than 0.9, there must be no isolated leptons and the Durhan jet resolution parameter $\log(y_{56})$ must be larger than -0.8. Then a likelihood discriminant is defined using as input the number of energy-flow objects, the second Fox-Wolfram moment, the event sphericity, the thrust, the jet resolution parameters y_{34} and y_{56}. Depending on the mass of the Higgs boson, events are accepted when the value of this discriminant is larger than a given threshold. The six jets are now grouped in three dijet pairs following criteria which depend on the mass of the Higgs boson. If $m_\mathrm{H} < 2m_\mathrm{W}$ only one W is expected to be on the mass shell. Therefor the quantity

$$\chi^2 = (m_\mathrm{ij} - m_\mathrm{Z})^2/\sigma_Z^2 + (m_\mathrm{kl} - m_\mathrm{W})^2/\sigma_W^2 \tag{4}$$

is calculated for all possible dijet combinations, where m_ij is the invariant mass of the two jets assigned to the Z and m_kl the invariant mass of two jets assigned to a W. The quantities σ_Z^2 and σ_W^2 are the convolution of the bosonic widths and the mass resolutions. They are estimated to be about 4 GeV. For $m_\mathrm{H} > 2m_\mathrm{W}$ both W bosons are on shell. Again all dijet combinations are taken and the quantity

$$\chi^2 = (m_\mathrm{ij} - m_\mathrm{Z})^2/\sigma_Z^2 + (m_\mathrm{kl} - m_\mathrm{W})^2/\sigma_W^2 + (m_\mathrm{mn} - m_\mathrm{W})^2/\sigma_W^2 \tag{5}$$

is calculated, where m_mn is the mass of the two jets stemming from the second W.

The jet pairing with the smallest value of χ^2 is chosen and subject of a kinematic fit imposing energy-momentum conservation and constraining the mass of the two

TABLE 2. Uncertainties on the determination of m_{H} and the cross sections, for m_{H} = 120, 150 and 180 GeV.

Decay mode	Δm_{H} in MeV			$\Delta\sigma/\sigma$ in %		
	120	150	180	120	150	180
recoil mass	110	90	95	2.6	3.2	3.8
$\mathrm{ZH} \to \ell^+\ell^-\mathrm{q\bar{q}}$	70	90	–	3.0	4.7	–
$\mathrm{ZH} \to \mathrm{q\bar{q}b\bar{b}}$	45	170	–	1.1	3.4	–
$\mathrm{ZH} \to \ell^+\ell^-\mathrm{W^+W^-},\ \mathrm{W^\pm} \to \mathrm{q\bar{q}'}$	310	95	100	13.0	5.2	4.0
$\mathrm{ZH} \to \mathrm{q\bar{q}W^+W^-},\ \mathrm{W^\pm} \to \mathrm{q\bar{q}'}$	250	100	110	12.0	4.6	4.4
Combined	$\simeq$ 40	$\simeq$ 50	$\simeq$ 70	$\simeq$1	$\simeq$2	$\simeq$ 3

jets stemming from the Z to m_{Z}. The selection efficiency for the signal is 4%, 30% and 21% for m_{H} = 120, 150 and 180 GeV, respectively. The distributions of the invariant mass of the 4-jet system is shown in Figure 6 for m_{H} = 150 GeV and 180 GeV, respectively.

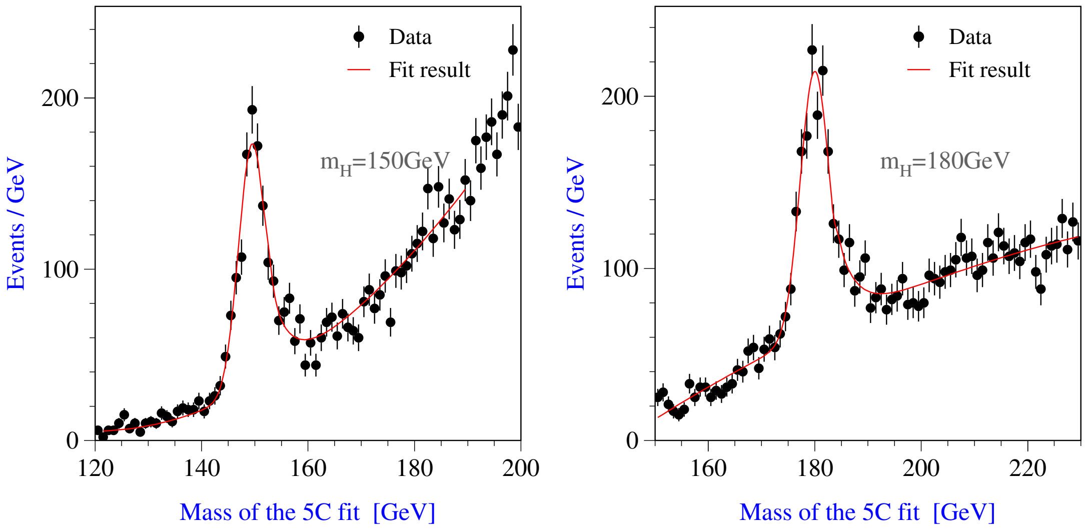

FIGURE 6. The four jet invariant mass from the $\mathrm{ZH} \to \mathrm{q\bar{q}W^+W^-}$ final state after a 5C kinematic fit for m_{H} = 150 GeV (left) and m_{H} = 180 GeV (right).

From a fit with a Gaussian the uncertainty of the mass is about 100 MeV and of the the cross section about 4% for both mass values.

SUMMARY

Table 2 summarises the accuracy on the determination of m_{H} for the different final states and their combination, for Higgs boson masses of 120, 150 and 180 GeV. The relative uncertainties of the cross section are also listed in Table 2.

REFERENCES

1. S.L. Glashow, Nucl. Phys. **22** (1961) 579; S. Weinberg, Phys. Rev. Lett. **19** (1967) 1264; A. Salam, *Elementary Particle Theory*, edited by N. Svartholm (Almqvist and Wiksell, Stockholm, 1968), p. 367.
2. P.W. Higgs, Phys. Lett. **12** (1964) 132, Phys. Rev. Lett. **13** (1964) 508 and Phys. Rev. **145** (1966) 1156 ; F. Englert and R. Brout, Phys. Rev. Lett. **13** (1964) 321; G.S. Guralnik, C.R. Hagen and T.W.B. Kibble, Phys. Rev. Lett. **13** (1964) 585.
3. "Conceptual Design of a 500 GeV e^+e^- Linear Collider with Integrated X-ray Laser Facility", Vol. I, editors R. Brinkmann, G. Materlik, J. Rossbach, A. Wagner, DESY 1997-048, ECFA 1997-182.
4. SIMDET V3.2, M. Pohl and H.J. Schreiber, DESY-99-030 (1999).
5. PYTHIA V6.136, T. Sjöstrand, Comp. Phys. Comm. **82** (1994) 74.
6. F.A. Berends, R. Kleiss and R. Pittau, Comp. Phys. Comm. **85** (1995) 437.
7. CIRCE V6, T. Ohl, Comp. Phys. Comm. **94** (1996) 53.
8. P. Garcia-Abia and W. Lohmann, EPJdirect **C2** (2000) 1-6.
9. J.C. Brient, LC-PHSM-2000-049-TESLA (2000).
10. S. Jadach *et al.*, Phys. Rev. **D 40** (1989) 3582, Comp. Phys. Comm. **70** (1992) 305, Phys. Lett. **B 390** (1997) 298.
11. Yu.L. Dokshitzer, G.D. Leder, S. Moretti and B.R. Webber, Cavendish-HEP-97/06.
12. S. Catani *et al.*, Phys. Lett. **B 269** (1991) 432;
    S. Bethke *et al.*, Nucl. Phys. **B 370** (1992) 310.
13. V. Blobel, "Constrained Least Squares and Error Propagation", Hamburg (1997).
14. R. Hawkings, LC note LC-PHSM-2000-021-TESLA (2000); K. Desch, private communication.
15. A. Raspereza, LC note, in preparation;